

AMCoR

Asahikawa Medical University Repository <http://amcor.asahikawa-med.ac.jp/>

Molecular carcinogenesis (2012.Aug) 21:.

Serine 727 phosphorylation of STAT3: An early change in mouse hepatocarcinogenesis induced by neonatal treatment with diethylnitrosamine

Miyakoshi M, Yamamoto M, Tanaka H, Ogawa K

Serine 727 Phosphorylation of STAT3: An Early Change in Mouse Hepatocarcinogenesis Induced by Neonatal Treatment with Diethylnitrosamine

Masaaki Miyakoshi¹, Masahiro Yamamoto¹, Hiroki Tanaka^{1,2} and Katsuhiko Ogawa^{1*}

¹*Department of Pathology, Section of Oncology, Asahikawa Medical University, Asahikawa, Japan*

²*Division of Pathological Biochemistry, Department of Biomedical Sciences, School of Life Science, Faculty of Medicine, Tottori University, Yonago, Japan*

Short title: *STAT3 ACTIVATION IN MOUSE HEPATOCARCINOGENESIS*

Abbreviations: HCC, hepatocellular carcinoma; DEN, diethylnitrosamine; FBS, fetal bovine serum; PD, PD98059; LY, LY294002; JKI, JAK kinase inhibitor 1

*Correspondence should be addressed to Katsuhiko Ogawa: Department of Pathology, Section of Oncology, Asahikawa Medical University, 2-1-1-1, Midorigaoka East, Asahikawa 078-8510, Japan. E-mail: ogawak@asahikawa-med.ac.jp.

ABSTRACT

STAT3 activation is involved in development and progression of human cancers, including hepatocellular carcinoma (HCC). We investigated STAT3 activation during multiple-stage hepatocarcinogenesis induced by neonatal diethylnitrosamine (DEN) treatment in mice. Nuclear accumulation and phosphorylation of STAT3 were detected in altered hepatocyte foci in the early stages as well as adenomas and HCCs in the late stages. Although total STAT3 levels were the same between the hepatic lesions and normal livers, S727-phosphorylated STAT3 was enhanced in adenomas and HCCs, whereas Y705-phosphorylated STAT3 was detected mainly in HCCs. In mouse HCC cell lines, although both S727 and Y705 remained un- or hypophosphorylated under serum-free conditions, fetal bovine serum (FBS) induced strong S727/no or weak Y705 phosphorylation, STAT3 nuclear accumulation and cell proliferation, whereas IL-6 treatment without FBS caused Y705 phosphorylation without S727 phosphorylation, STAT3 nuclear accumulation or cell proliferation. When HCCs were simultaneously treated with FBS/IL-6, selective suppression of S727 phosphorylation by a MEK inhibitor prevented STAT3 nuclear accumulation and cell proliferation. Furthermore, a S727 phosphorylation-deficient STAT3 mutant (S727A) had a diminished capacity to accumulate in the nucleus when compared with wild-type (WT) or the phosphorylation-mimic mutant (S727D) following treatment with FBS/IL-6. After treatment with FBS/IL-6, the cells expressing the S727A mutant proliferated more slowly than those expressing WT or S727D mutant. In contrast, suppression of Y705 phosphorylation by a JAK inhibitor in the FBS/IL-6 treated cells did not affect STAT3 nuclear accumulation or cell proliferation. Taken together, these data demonstrate that STAT3 activation, mainly through S727 phosphorylation, contributes to the DEN-induced hepatocarcinogenesis at the earliest stages.

Key words: preneoplastic hepatocytes, STAT3, S727 phosphorylation, Y705 phosphorylation, DEN-induced hepatocarcinogenesis

INTRODUCTION

Hepatocellular carcinoma (HCC) is the fifth most common human cancer and the third most common cause of cancer deaths worldwide [1]. Geographically, HCC patients are distributed mainly in Asia and Africa. HCC frequently presents clinical signs and symptoms during the late stage of the disease, resulting in poor prognosis and a high mortality rate [2]. The main risk factor for HCC is chronic liver injury due to hepatitis B or C virus infection, alcohol abuse or non-alcoholic hepatic steatosis. Because it generally takes anywhere from 20 to 40 years for HCC to manifest in injured livers, appropriate intervention might prevent the development and progression of HCC.

In chemically induced hepatocarcinogenesis, altered hepatocyte foci consisting of preneoplastic hepatocytes emerge during the early stage of the disease [3]. These preneoplastic hepatocytes are thought to be the proximal descendants of initiated cells that had been transformed from normal hepatocytes at a low frequency through genetic alterations. These cells are distinct from normal hepatocytes because they exhibit high proliferation rates and enhanced survival capacities, especially in the chronically injured hepatic environment. These cells can progress to adenoma cells presumably through additional genetic alterations, and HCC cells may ultimately arise from adenoma cells.

Inappropriate STAT3 activation frequently occurs in a variety of human cancers, including HCC [4, 5]. STAT3 can be activated via the actions of various upstream protein kinases, such as JAK, EGF receptor and Src, or it can be activated through the impairment of a STAT3 negative regulator, such as SOCS3 [6]. Phosphorylation of the tyrosine 705 residue (Y705) in STAT3 results in the formation of a STAT3 homodimer or a STAT3/STAT1 heterodimer that can bind to specific DNA response elements in the promoter regions of target genes and induce unique gene expression programs [6]. Phosphorylation of serine 727 (S727) also contributes to the maximal

transcriptional activity of STAT3. In addition to the Y705-dependent activation, under certain conditions, STAT3 can also be activated through Y705 phosphorylation-independent mechanisms [7-9].

Disruption of STAT3 in HCC cells has been shown to result in increased apoptosis and retarded growth [10-12], indicating that survival and proliferation of HCC cells depend on STAT3. In contrast, constitutive STAT3 activation in hepatocytes has been demonstrated to promote hepatocarcinogenesis in mice [13-15], whereas STAT3 inactivation in hepatocytes suppresses hepatocarcinogenesis [16]. Furthermore, constitutive activation of STAT3 due to activating mutations in *STAT3* or *gp130*, which encodes a cytokine coreceptor that mediates STAT3 activation by certain cytokines, has been detected in human hepatocellular adenomas [17, 18]. These findings indicate that STAT3 activation plays an important role in hepatocarcinogenesis.

In humans, hepatocarcinogenesis is usually associated with chronic hepatitis or liver cirrhosis which may be due to viral or nonviral causes [2]. In these cases, the hepatic tissue microenvironment is enriched with cytokines, growth factors and reactive oxygen species that are produced by the hepatic and inflammatory cells. These factors continuously activate STAT3, which stimulates the proliferation and survival of preneoplastic and neoplastic hepatocytes [19, 20]. Indeed, hepatocarcinogenesis in mice has been shown to be enhanced under conditions associated with persistent hepatic injury, inflammation and steatosis [21-27].

However, studies using a mouse hepatocarcinogenesis model generated by the treatment of neonatal B6C3F1 mice with a single dose of DEN observed no pathological changes in the liver tissue surrounding the tumor, and preneoplastic hepatocytes spontaneously progressed into HCC cells without any further treatment [28]. Importantly, it is not known if STAT3 activation is involved in this hepatocarcinogenesis model without

associated hepatic injury in the surrounding non-neoplastic hepatic tissues. In the current study, we found that STAT3 was activated at a very early stage in the DEN-induced hepatocarcinogenesis model and that STAT3 phosphorylation occurred through a two-step process; S727 phosphorylation was increased during the preneoplastic stage, whereas Y705 phosphorylation was mainly associated with malignant progression. We further investigated the factors and pathways involved in STAT3 activation and the role of STAT3 using mouse cell lines derived from DEN-induced HCCs.

MATERIALS AND METHODS

Tissues, Cell Lines and Other Materials

Two-week-old male B6C3F1 mice were treated with DEN (5 $\mu\text{g/g}$ body weight) and sacrificed 5, 10 and 15 months later. For histological and immunohistochemical examination, the liver tissues were fixed in 10% buffered formalin and embedded in paraffin. For biochemical analysis, the grossly visible tumors were dissected from the surrounding liver tissue, and half of the tissue was examined histologically, and the other half was snap frozen in liquid nitrogen and stored at -80°C until further analysis. Histological criteria for mouse hepatic tumors have been previously described [29]. All animal procedures were approved by the Asahikawa Medical College committee and were performed according to the guidelines for the humane care of laboratory animals. The mouse HCC cell lines (HCC8 and HCC3), which were established from DEN-induced HCCs [30, 31], were cultured in Williams' E medium (Sigma, St. Louis, MO) supplemented with 10% fetal bovine serum (FBS) at 37°C in a humidified incubator with a constant air flow containing 5% CO_2 . The JAK kinase inhibitor I (JKI) and PD98059 (PD) were purchased from Calbiochem (San Diego, CA), and LY294002 (LY) was purchased from Sigma. These inhibitors were used by adding to the culture medium at the concentrations of 2 μM for JKI, 50 μM for PD and 40 μM

for LY, respectively. The antibodies used in the studies were against the following proteins: α -tubulin, lamin A (Santa Cruz Biotechnology, Santa Cruz, CA), STAT3, phospho-STAT3, Akt, phospho-Akt, ERK1/2, phospho-ERK1/2, hemagglutinin (HA) (Sigma), F4/80 (Abcam, Cambridge, UK) and Ki-67 (DAKO, Carpinteria, CA).

Immunoblot Analysis

Protein lysates were run on polyacrylamide gels containing 0.1% sodium dodecyl sulfate and transferred to Hybond-P PVDF membranes (GE Healthcare, UK). The membranes were probed with appropriate primary antibodies and then hybridized with horseradish peroxidase-conjugated anti-mouse or anti-rabbit immunoglobulin (GE Healthcare). The bound antibodies were detected using the ECL Plus kit (GE Healthcare).

Cell Fractionation

Nuclear and cytoplasmic fractions of the HCC cells were obtained using the NE-PER kit (Pierce, Rockford, IL) according to the manufacturer's instructions.

Immunohistochemistry and Immunofluorescence

Antigen retrieval of the tissue sections was performed in an autoclave using a solution containing 0.01 M citrate and 0.1% NP-40, and the sections were incubated with primary antibodies overnight at 4°C . Antibody binding was detected using the Catalyzed Signal Amplification System II (DAKO). For immunofluorescence, cryostat sections of the hepatic tissues or the HCC cells grown on collagen-coated coverslips were fixed in 10% formalin and incubated overnight with primary antibodies. The cells were then incubated with rhodamine- or FITC-conjugated anti-mouse or anti-rabbit antibodies, stained with DAPI and examined using a fluorescence microscope.

In Vitro Growth Assays

For the *in vitro* cell growth assay, a total of 10^5 cells were seeded in collagen-coated 6-well plates, harvested using a trypsin-EDTA solution and stained with trypan blue. The cells were examined under a microscope, and the number of viable cells was determined using a hemocytometer. The *in vitro* assay was performed in triplicate, and the experiments were repeated at least three times.

Wild-Type, S727 Phosphorylation-Dead and S727 Phospho-Mimic STAT3 Constructs

Wild-type (WT) STAT3 cDNA was tagged at the 5' end with an HA epitope and cloned into the pCI neo vector (Invitrogen, Carlsbad, CA). The S727 phosphorylation-dead STAT3 mutant (S727A) in which S727 was replaced with alanine, and the S727 phosphorylation-mimic STAT3 mutant (S727D) in which S727 was replaced with aspartic acid [32], were generated from the WT vector using a site-directed mutagenesis kit (Invitrogen) according to the manufacturer's instructions. The WT, S727A and S727D vectors were transfected into HCC8 cells using Lipofectamine 2000 (Invitrogen) at a confluency of 70-80%. The transfected cells were cultured in medium containing 10% FBS and 10 ng/ml IL-6 or IL-6 alone for 48 hr. The cells were then fixed in 1% buffered formalin and stained for immunofluorescence of HA and Ki-67.

Statistical Analysis

The data in the bar graphs are presented as the mean \pm SD. The means were analyzed using a Student's *t*-test, and *p* values of less than 0.05 were considered statistically significant.

RESULTS

STAT3 Activation During the DEN-Induced Hepatocarcinogenesis

Five months after the treatment of neonatal B6C3F1 mice with DEN (5 μ g/g body weight), their livers contained altered hepatocyte foci (Figure 1A, a) and small adenomas (less than 3 mm in diameter) (Figure 1A, b). After 10 months, large adenomas (more than 5 mm in diameter), foci, and small adenomas were observed, and at 15 months, HCCs were found alongside the adenomas (Figure 1A, c). Histologically, the unaffected liver tissue was normal; no pathological changes, such as inflammation, fibrosis or steatosis, were observed at 5 or 10 months (Figure 1A, a and b). At 15 months, necrotic areas infiltrated with inflammatory cells (mainly F4/80-positive macrophages) were occasionally found within HCCs (Figure 1A, c and d). Immunoblot results showed that total STAT3 (STAT3 α) levels remained unchanged between normal liver tissue, adenomas and HCCs. However, S727-phosphorylated STAT3 was markedly increased in all adenomas ($n=10$) and HCCs ($n=10$) when compared with normal liver tissue ($n=5$) (partially shown in Figure 1B). In contrast, Y705-phosphorylated STAT3 was much more increased in HCCs than adenomas (Figure 1B). Because various cellular signaling pathways had been reported to lead to S727 phosphorylation (7), we investigated whether ERK and Akt activation was associated with the increased S727 phosphorylation in hepatic tumors. ERK was weakly phosphorylated in some but not all hepatic tumors, while Akt was highly phosphorylated in all adenomas and HCCs (Figure 1B). Upon immunohistochemical staining and immunofluorescence analysis, total STAT3 (Figure 1C, a, b and c) and phospho-STAT3 (S727) (Figure 1C, d and e) were detected in the nuclei of the hepatocytes in foci ($n=8$), adenomas ($n=10$) and HCCs ($n=6$), but they were not observed in the nuclei of surrounding normal hepatocytes. There was no STAT3 nuclear staining when the primary antibody was omitted (data not shown).

never induced S727 phosphorylation at these doses (data not shown). In contrast, when the cells were treated with 10% FBS, S727 was hyperphosphorylated, whereas Y705 phosphorylation was only weakly enhanced in HCC8 cells and unchanged in HCC3 cells (Figure 2). When the cells were simultaneously treated with 10% FBS and 10 ng/ml IL-6, both Y705 and S727 were hyperphosphorylated in both cell lines (Figure 2). Phosphorylation of ERK and Akt was also enhanced in both cell lines when treated with FBS or FBS/IL-6 (Figure 2).

Figure 1 Histology of hepatic lesions and STAT3 activation in DEN-induced hepatocarcinogenesis. (A) Focus (Fc) (a), adenoma (Ad) (b) and HCC (c). The selected area of HCC (c) containing F4/80-positive macrophages (d). Note that no pathological changes were observed in the normal liver tissue surrounding the focus (a) and adenoma (b). (B) Immunoblot analysis using antibodies recognizing total or phospho-STAT3, total or phospho-ERK and total or phospho-Akt in normal liver (Nor), adenomas (Ad) and HCCs. α -tubulin was used as a loading control. (C) STAT3 nuclear staining in the hepatocytes of the focus (Fc) (a, d), adenoma (Ad) (b) and HCC (c, e). An antibody recognizing total STAT3 was used for panels a-c, and an antibody recognizing phospho-STAT3 (S727) was used for panels d and e.

Induction of STAT3 Phosphorylation in Mouse HCC Cells

Because STAT3 activation is usually dependent on extracellular signals, such as cytokines and growth factors [6], we investigated the factors that mediated STAT3 phosphorylation using the HCC8 and HCC3 cell lines, which were derived from DEN-induced mouse HCCs [30, 31]. Following serum starvation for 24 hr, both S727 and Y705 were un- or hypophosphorylated in both cell lines (Figure 2). When the cells were treated with 10 ng/ml IL-6 after 24 hr of serum starvation, STAT3 in both cell lines was hyperphosphorylated at Y705 within 60 min, but there was no increase in S727 phosphorylation (Figure 2). The degree of Y705 phosphorylation reached its maximum level following treatment with 5-50 ng/ml IL-6, but IL-6

Figure 2 Induction of phosphorylation of STAT3, ERK and Akt in HCC8 and HCC3 cells upon treatment with IL-6, FBS or IL-6 and FBS after serum starvation for 24 hr.

Signaling Pathways Involved in STAT3 Phosphorylation

In the cells treated with both FBS and IL-6, STAT3 Y705 phosphorylation was inhibited by treatment with the JAK kinase inhibitor, JKI, in both cell lines, but there was no change in the phosphorylation at S727 (Figure 3). Conversely, STAT3 S727 and ERK phosphorylation were inhibited by treatment with the MEK inhibitor, PD, without a change in STAT3 Y705 phosphorylation (Figure 3). When the FBS and IL-6-treated cells were treated with the PI3K inhibitor, LY, there was no change in STAT3 phosphorylation at either Y705 or S727 despite the inhibition of Akt phosphorylation observed in both cell lines (Figure 3). Therefore, Y705 and S727 phosphorylation were dependent on JAK and MEK activation, respectively, whereas the PI3K-Akt pathway

played no role in STAT3 phosphorylation in either cell line.

Figure 3 Signaling pathways involved in STAT3 phosphorylation in HCC8 and HCC3 cells. Phosphorylation status of STAT3 at Y705, STAT3 at S727, ERK and Akt after a 60 min treatment of the serum-starved cells with IL-6 and FBS in the presence or absence of JKI, PD or LY.

Correlation between S727 Phosphorylation and STAT3 Nuclear Accumulation

Because the nuclear accumulation of STAT3 suggests an increase in its transcriptional activity [6], we investigated the correlation between STAT3 phosphorylation and its nuclear accumulation in the HCC8 cells that showed a flat polygonal morphology. After a 24-hr serum starvation period, STAT3 was mainly localized to the cytoplasm as detected using immunofluorescence staining (Figure 4A, a). Although STAT3 was also detected mainly in the cytoplasm following treatment of the serum-starved cells with 10 ng/ml IL-6 (Figure 4A, b), it was localized to both the nucleus and the cytoplasm within 60 min of treatment with 10% FBS (Figure 4A, c). When the serum-starved cells were treated simultaneously with FBS and PD for 60 min, the FBS-induced nuclear accumulation of STAT3 was inhibited (Figure 4A, d), suggesting that the nuclear accumulation of STAT3 correlated with its phosphorylation at S727. In contrast, when the serum-starved cells were treated simultaneously with FBS and either JKI (Figure 4A, e) or LY (Figure 4A, f), the FBS-induced nuclear accumulation of STAT3 was intact,

indicating that this process was not linked to its phosphorylation at Y705 or to the activation of the PI3K-Akt pathway. To confirm the immunofluorescence results, cytoplasmic and nuclear fractions were isolated from the HCC8 cells, and the cytoplasmic and nuclear distribution of STAT3 was examined by immunoblotting (Figure 4B). When the antibody against total STAT3 was used, although STAT3 was detected in both the cytoplasmic and nuclear fractions of the serum-starved cells, the levels of nuclear STAT3 increased following treatment with FBS, but not with IL-6, when expression levels were normalized to the levels of the nuclear protein, lamin A (Figure 4B). When the phosphorylation-specific STAT3 antibodies were used instead of the antibody against total STAT3, nuclear S727 phospho-STAT3 was shown increased by FBS treatment, while small amounts of Y705 phospho-STAT3 detected in the nuclear fractions was unchanged in the same conditions (Figure 4B, b). In support of the immunofluorescence results, the FBS-induced nuclear accumulation of STAT3 was inhibited by treatment with PD, but not by treatment with JKI or LY (Figure 4B, a and b).

Figure 4 Nuclear accumulation of STAT3 in HCC8 cells. (A) STAT3 distribution after a 24-hr serum starvation period (a) and following treatment of the serum-starved cells with IL-6 (b), FBS (c), FBS plus PD (d), JKI (e) or LY (f). (B) Immunoblot analysis of STAT3 and lamin A in cytoplasmic (c) and nuclear (n) fractions of HCC8 cells and densitometric

analysis of nuclear STAT3 vs. lamin A. Upper panel: Total STAT3, lower panel: Phospho-Y705 and S727 STAT3.

Correlation between STAT3 S727 Phosphorylation and Cell Proliferation

Treatment of the serum-starved HCC cells with 10% FBS for 4 days increased HCC8 cell numbers eight-fold (Figure 5A, a) and HCC3 cells 35-fold (Figure 5A, b), whereas treatment with 10 ng/ml IL-6 alone did not increase cell numbers in either cell line (Figure 5A, a and b). When compared to treatment with FBS alone, simultaneously treating the cells with FBS and IL-6 increased the cell numbers significantly in HCC8 cells ($p < 0.05$) (Figure 5A, a and 5B, a) and slightly increased the cell numbers in HCC3 cells (Figure 5A, b). When HCC8 cells were treated with various concentrations of FBS or IL-6, the increase in the cell number was dependent on the FBS, but not the IL-6 concentration, although IL-6 weakly synergized with FBS (Figure 5B, a and b). When used with FBS and IL-6, PD markedly inhibited the increase in cell number in both cell lines, whereas the cell number was not affected by JKI treatment (Figure 5C, a and b), suggesting that S727 phosphorylation, but not Y705 phosphorylation, of STAT3 is important for cell proliferation. Similarly, inhibition of the PI3K-Akt pathway by LY in the FBS and IL-6-treated cells resulted in the suppression of cell proliferation (Figure 5C, a and b), although it did not inhibit STAT3 phosphorylation (Figure 3).

Figure 5 Proliferation of HCC8 and HCC3 cells. (A) HCC8 (a) and HCC3 (b) cell numbers during 4 days without FBS and IL-6 treatment and in the presence of IL-6, FBS or FBS and IL-6. * $p < 0.05$. (B) The increase in HCC8 cell number following treatment with various concentrations of FBS in the presence (closed bars) or absence (open bars) of 10 ng/ml IL-6 ($p < 0.05$) (a) and treatment with various concentrations of IL-6 in the presence (closed bars) or absence (open bars) of 10% FBS for 4 days (b). (C) HCC8 (a) and HCC3 (b) cell numbers 4 days after treatment with FBS and IL-6 in the presence or absence of JKI, PD or LY.

The Effects of WT, S727A and S727D STAT3 Expression in HCC Cells

The above data indicated that S727 phosphorylation of STAT3 correlated with STAT3 nuclear accumulation and cell proliferation. To further investigate the role of S727 phosphorylation, HCC8 cells were transfected with a plasmid carrying the HA-tagged WT, S727 phosphorylation-deficient S727A or S727 phosphorylation-mimic S727D versions of STAT3 [32]. The transfected cells were examined for nuclear accumulation of the HA-tagged STAT3 and cell proliferation. After transfection, the cells were cultured for 48 hr with or without FBS and IL-6 and analyzed for immunofluorescence after staining with DAPI and antibodies against HA and Ki-67. Approximately 30-40% of the cells were positive for HA, indicating that

these cells expressed the STAT3 proteins encoded by the constructs (Figure 6A, B). In the condition with FBS and IL-6, the nuclear localization of the HA-tagged STAT3 protein in the cells expressing S727A was significantly reduced when compared with the cells expressing WT or S727D STAT3 (Figure 6A, a). There were also significantly fewer nuclear Ki-67-positive cells among the cells expressing S727A when compared with the cells expressing WT or S727D STAT3 (Figures 6B, a). On the other hand, under the condition without FBS and IL-6, although Ki-67 index was low in the cells expressing a S727D mutant as well as those expressing WT or S727A STAT3 (Figure 6B, b), nuclear accumulation of S727D was much more increased as compared to WT and S727A STAT3 (Figure 6A, b), indicating that S727 phosphorylation-mimic S727D STAT3 could accumulate in the nucleus, although it could not enhance cell proliferation.

accumulation of HA-tagged WT, S727A or S727D STAT3 (** $p < 0.01$, * $p < 0.05$). (a) FBS(+)/IL-6(+), (b) FBS(-)/IL-6(-). (B) Immunofluorescence of HA-tagged WT, S727A and S727D STAT3 (green) and Ki-67 (red) and percentage of the Ki-67-positive cells expressing HA-tagged WT, S727A or S727D STAT3 (** $p < 0.01$, * $p < 0.05$). Arrowheads in above panels indicate the Ki-67-positive cells among the HA-positive cells. (a) FBS(+)/IL-6(+), (b) FBS(-)/IL-6(+).

DISCUSSION

Our study demonstrated that in hepatocarcinogenesis induced by neonatal treatment of male B6C3F1 mice with DEN, STAT3 was activated at the earliest stage of the disease. Furthermore, STAT3 activation occurred by a two-step process during the progression of hepatocarcinogenesis; STAT3 S727 phosphorylation was observed at the preneoplastic stage, and phosphorylation at Y705 of STAT3 was mainly detected in association with malignant progression. In HCC cell lines derived from DEN-induced HCCs, STAT3 was un- or hypophosphorylated in the absence of serum; however, treatment with FBS significantly enhanced S727 phosphorylation of STAT3 with weak or no increase of Y705 phosphorylation, whereas treatment with IL-6 specifically induced Y705 phosphorylation of STAT3. These data suggest that STAT3 activation in hepatocarcinogenesis depends on factor(s) that are physiologically present in the serum or hepatic tissue environment. The factors potentially responsible for the selective S727 phosphorylation include colony-stimulating factors [33], leptin [34], insulin [35] and insulin-like growth factors [36]. Y705 phosphorylation might be achieved by cytokines, such as IL-6, that are produced by HCC cells [37] and inflammatory cells infiltrated within the HCC tissues. Because it has been demonstrated that Y705 and S727 phosphorylation synergistically induce the full transcriptional capability of STAT3 [6], the additional Y705 phosphorylation in HCC cells may result in increased STAT3 transcriptional activity, which may impact increased neoplastic properties to the HCC cells. This hypothesis is supported by the fact that the simultaneous treatment of HCC cells with FBS and IL-6

Figure 6 Expression of WT, S727A and S727D STAT3 in HCC8 cells. (A) Nuclear accumulation (arrowheads) of HA-tagged WT, S727A or S727D STAT3 (green) and percentage of cells that displayed nuclear

weakly enhanced cell proliferation when compared with treatment of the same cells with FBS alone.

In the HCC cells treated with FBS and IL-6, S727 phosphorylation of STAT3 was specifically suppressed by PD, whereas Y705 phosphorylation of STAT3 was specifically suppressed by JKI, indicating that S727 phosphorylation is dependent on MEK activation, and Y705 phosphorylation is dependent on JAK activation. The MEK inhibitor (PD) strongly suppressed cell proliferation and S727 phosphorylation of STAT3 in FBS/IL-6 treated cells, and the FBS/IL-6 treated cells expressing the phosphorylation-dead S727A mutant STAT3 were significantly less proliferative when compared with the cells expressing WT STAT3 or the phosphorylation-mimic S727D mutant STAT3. These observations indicate that phosphorylation of STAT3 at S727 is likely linked to cell proliferation. Conversely, inhibition of Y705 phosphorylation by JKI in the cells treated with FBS and IL-6 did not affect cell proliferation, indicating that Y705 phosphorylation of STAT3 is less important for cell proliferation in the HCC cells. The functional importance of S727 phosphorylation, independent of Y705 phosphorylation, has been demonstrated in a number of phenomena, such as the FBS-induced activation of macrophages [38], the proliferation of a human prostate carcinoma cell line, LNCaP [32], postnatal survival and growth in mice [39], Notch-mediated neuronal stem cell survival [40] and the amino acid-mediated inhibition of insulin signaling in HepG2 cells [41]. S727-phosphorylated STAT3, therefore, is thought to play an important role from the earliest stage of hepatocarcinogenesis. On the other hand, although the MEK-ERK pathway was indicated responsible for S727 phosphorylation in the HCC cell lines *in vitro*, ERK phosphorylation was only weakly increased in some but not all hepatic tumors *in vivo*. So, the exact mechanism of S727 phosphorylation in the hepatic tumors *in vivo* requires further investigations.

It is generally accepted that Y705 phosphorylation is a prerequisite for the nuclear localization of STAT3 [6]. However, in our present study, the MEK inhibitor (PD) suppressed the FBS-induced nuclear accumulation of STAT3 as well as the S727 phosphorylation of STAT3. Moreover, the S727 phosphorylation-deficient S727A mutant exhibited a decreased accumulation in the nucleus after treatment with FBS and IL-6 compared with WT STAT3 and the S727D mutant, and S727D STAT3 accumulated in the nucleus more than WT and S727A STAT3 in the absence of FBS and IL-6, indicating that phosphorylation at S727 is important for the nuclear accumulation of STAT3 in the HCC cells. On the other hand, suppression of Y705 phosphorylation by the JAK inhibitor in the FBS-IL-6 treated cells did not remarkably inhibit STAT3 nuclear accumulation. It has been demonstrated that unphosphorylated STAT3 continuously shuttles between the cytoplasm and nucleus under steady state conditions in an importin α 3-dependent manner, and the degree of nuclear accumulation of STAT3 is dependent on the cell type and extracellular signals [42]. Additionally, the nuclear accumulation of STAT3 has been detected in some tumors and primary cells independently of Y705 phosphorylation [43]. On the other hand, in the present study, although the S727D phosphorylation-mimic STAT3 could accumulate in the nucleus in the condition without FBS and IL-6, it did not stimulate cell proliferation, suggesting that certain serum factor(s) are required for cell proliferation in addition to STAT3 S727 phosphorylation.

In summary, our study demonstrated that phosphorylation of STAT3 at S727 occurred at or before the preneoplastic stage during DEN-induced mouse hepatocarcinogenesis, suggesting that the preneoplastic hepatocytes gain their growth and survival advantage over normal hepatocytes, at least in part, through STAT3 activation. In contrast, the phosphorylation of STAT3 at Y705 mainly occurred in association with malignant progression, suggesting that the HCC cells further increase their tumorigenic potential through the increased

phosphorylation at Y705. Based on the results of this study, STAT3 may be a crucial target for the prevention of hepatocarcinogenesis.

ACKNOWLEDGEMENTS

This study was supported by grants from the Japanese Ministry of Education, Science, Culture and Sports and grants from the Asahikawa Medical College Advanced Science Research Program.

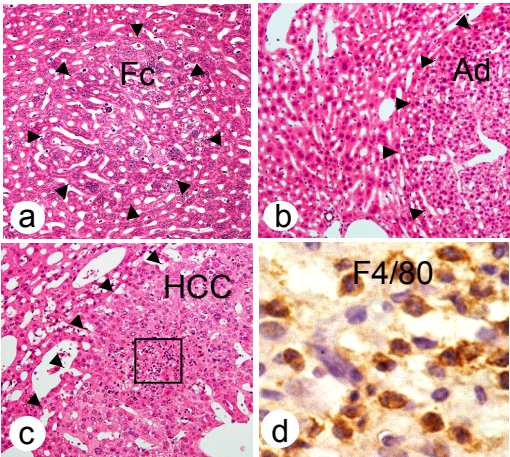
REFERENCES

1. Tabor E. Hepatocellular carcinoma: global epidemiology. *Dig Liver Dis* 2001;132:2557-2576.
2. Nordenstedt H, White DJ, El-Serag HB. The changing pattern of epidemiology in hepatocellular carcinoma. *Dig Liv Dis* 2010;42S:S206-S214.
3. Ogawa K. Molecular pathology of early stage chemically induced hepatocarcinogenesis. *Pathol Int* 2009; 59:605-622.
4. Damell Jr JE. Validating Stat3 in cancer therapy. *Nat Med* 2005;11:595-596.
5. Yu H, Pardoll D, Jove R. STATs in cancer inflammation and immunity: a leading role for STAT3. *Nat Rev Cancer* 2009;9:798-809.
6. Levy DE, Damell Jr JE. Stats: transcriptional control and biological impact. *Nat Rev Mol Cell Biol* 2002;3:651-662.
7. Decker T, Kovarik P. Serine phosphorylation of STATs. *Oncogene* 2000;19:2628-2637.
8. Yang J, Stark GR. Roles of unphosphorylated STATs in signaling. *Cell Res* 2008;18:443-451.
9. Grivennikov S, Karin M. Dangerous liaisons: STAT3 and NF- κ B collaboration and crosstalk in cancer. *Cytokine Growth Factor Rev* 2010;21:11-19.
10. Liu Y, Li PK, Li C, Lin J. Inhibition of STAT3 signaling blocks the anti-apoptotic activity of IL-6 in human liver cancer cells. *J Biol Chem* 2010; 285:27429-27439
11. Li WC, Ye SL, Sun RX, et al. Inhibition of growth and metastasis of human hepatocellular carcinoma by antisense orlignucleotide targeting signal transducer and activator of transcription 3. *Clin Cancer Res* 2006;12:7140-7148.
12. Kusaba M, Nakao K, Goto T, et al. Abrogation of constitutive STAT3 activity sensitizes human hepatoma cells to TRAIL-mediated apoptosis. *J Hepatol* 2007;47:546-555.
13. Maione D, Carlo ED, Li W, et al. Coexpression of IL-6 and soluble IL-6R causes nodular regenerative hyperplasia and adenomas of the liver. *EMBO J* 1998;17:5588-5597.
14. Ogata H, Kobayashi T, Chinen T, et al. Deletion of the SOCS3 gene in liver parenchymal cells promotes hepatitis-induced hepatocarcinogenesis. *Gastroenterology* 2006;131:179-193.
15. Riehle KJ, Campbell JS, McMahan RS, et al. Regulation of liver regeneration and hepatocarcinogenesis by suppressor of cytokine signaling 3. *J Exp Med* 2008; 205:91-103.
16. Naugler WE, Sakurai T, Kim S, et al. Gender disparity in liver cancer due to sex differences in MyD88-dependent IL-6 production. *Science* 2007;317:121-124.
17. Rebouissou S, Amessou M, Couchy G, et al. Frequent in-frame somatic deletions activate gp130 in inflammatory hepatocellular tumors. *Nature* 2009;457:200-204.
18. Pilati C, Amessou M, Bihl MP, et al. Somatic mutations activating STAT3 in human inflammatory hepatocellular adenomas. *J Exp Med* 2011;208:1359-1366.
19. Grivennikov SI, Greten FR, Karin M. Immunity, inflammation, and cancer. *Cell* 2010;140:883-899.
20. Wang H, Lafdil F, Kong X, Gao B. Signal transducer and activator of transcription 3 in liver diseases: a novel therapeutic target. *Int J Biol Sci* 2011;7:536-550.
21. Park EJ, Lee JH, Yu GY, et al. Dietary and genetic obesity promote liver inflammation and tumorigenesis by enhancing IL-6 and TNF expression. *Cell* 2010;140:197-208.
22. He G, Yu GY, Temkin V, et al. Hepatocyte IKK β /NF- κ B inhibits tumor promotion and progression by preventing oxidative stress-driven STAT3 activation. *Cancer Cell* 2010;17:286-297.
23. Maeda S, Kamata H, Luo JL, Leffert H, Karin M. IKK β couples hepatocyte death to cytokine-driven compensatory

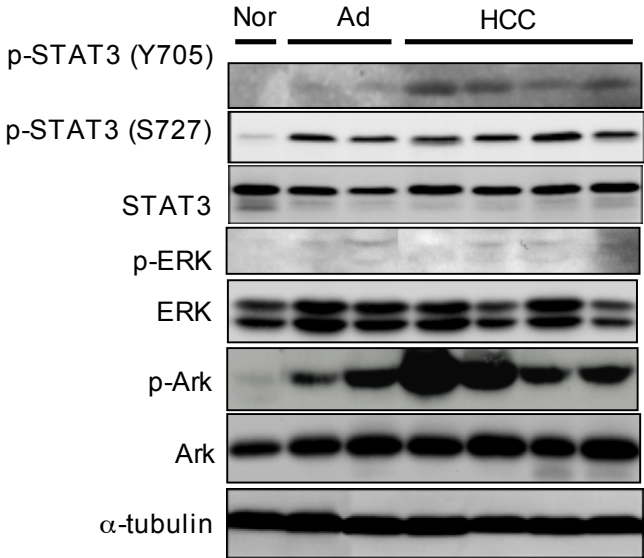
- proliferation that promotes chemical hepatocarcinogenesis. *Cell* 2005;121:977-990.
24. Luedde T, Beraza N, Kotsikris V, et al. Deletion of NEMO/IKK γ in liver parenchymal cells causes steatohepatitis and hepatocellular carcinoma. *Cancer Cell* 2007;11:119-132.
 25. Bard-Chapeau EA, Li S, Ding J, et al. Ptpn11/Shp2 acts as tumor suppressor in hepatocellular carcinogenesis. *Cancer Cell* 2011;19:629-639.
 26. Haybaek J, Zeller N, Wolf MJ, et al. A lymphotoxin-driven pathway to hepatocellular carcinoma. *Cancer Cell* 2009;16:295-308.
 27. Machida K, Tsukamoto H, Liu JC, et al. C-Jun mediates HCV hepatocarcinogenesis through STAT3 and nitric oxide-dependent impairment of oxidative DNA repair. *Hepatology* 2010;52:480-492.
 28. Vesselinovitch SD. Perinatal mouse liver carcinogenesis as a sensitive carcinogenesis model and the role of the sex hormonal environment in tumor development. *Prog Clin Biol Res* 1990;331:53-68.
 29. Thoolen B, Maronpot RR, Harada T, et al. Proliferative and nonproliferative lesions of the rat and mouse hepatobiliary system. *Toxicol Pathol* 2010;38:5S-81S.
 30. Yamamoto M, Tamakawa S, Yoshie M, Yaginuma Y, Ogawa K. Neoplastic hepatocyte growth associated with cyclin D1 redistribution from the cytoplasm to the nucleus in mouse hepatocarcinogenesis. *Mol Carcinog* 2006;45:901-913.
 31. Tanaka H, Yamamoto M, Hashimoto N, et al. Hypoxia-independent overexpression of hypoxia-inducible factor 1 α as an early change in mouse hepatocarcinogenesis. *Cancer Res* 2006;66:11263-11270.
 32. Qin HR, Kim HJ, Kim JY, et al. Activation of signal transducer and activator of transcription 3 through a phosphomimetic serine 727 promotes prostate tumorigenesis independent of tyrosine 705 phosphorylation. *Cancer Res* 2008;68:7736-77341.
 33. Valdembrì D, Serini G, Vacca A, Ribattu D, Bussolino F. *In vivo* activation of JAK2/STAT-3 pathway during angiogenesis induced by GM-CSF. *FASEB J* 2002;16:225-227.
 34. O'Rourke L, Shepherd PR. Biphasic regulation of extracellular-signal-regulated protein kinase by leptin in macrophages: role in regulating STAT3 Ser727 phosphorylation and DNA binding. *Biochem J* 2002; 364:875-879.
 35. Cerera BP, Pressin JE. Insulin stimulates the serine phosphorylation of the signal transducer and activator of transcription (STAT3) isoform. *J Biol Chem* 1996;271:12121-12124.
 36. Zong CS, Chan J, Levy DE, et al. Mechanism of STAT3 activation by insulin-like growth factor I receptor. *J Biol Chem* 2000;275:15099-15105.
 37. Soresi M, Giannitrapani L, D'Antona F, et al. Interleukin-6 and its soluble receptor in patients with liver cirrhosis and hepatocellular carcinoma. *World J Gastroenterol* 2006;12:2563-2568.
 38. Liu H, Ma Y, Cole SM, et al. Serine phosphorylation of STAT3 is essential for Mcl-1 expression and macrophage survival. *Blood* 2003;102:344-352.
 39. Shen Y, Schlessinger K, Zhu X, et al. Essential role of STAT3 in postnatal survival and growth revealed by mice lacking STAT3 serine phosphorylation. *Mol Cell Biol* 2004;24:407-419.
 40. Androutsellis-Theotokis A, Leker RR, Soldner F. Notch signaling regulates stem cell numbers in vitro and in vivo. *Nature* 2006;442:823-826.
 41. Kim JH, Yoon MS, Chen J. Signal transducer and activator of transcription 3 (STAT3) mediates amino acid inhibition of insulin signaling through serine 727 phosphorylation. *J Biol Chem* 2009;284:35425-35432
 42. Reich NC, Liu L. Tracking STAT nuclear traffic. *Nat Rev Immunol* 2006;6:602-612.
 43. Meyer T, Gavenis K, Vinkemeier U. Cell type-specific and tyrosine phosphorylation-independent nuclear presence of STAT1 and STAT3. *Exp Cell Res* 2002;272:45-55.

Figure 1

A



B



C

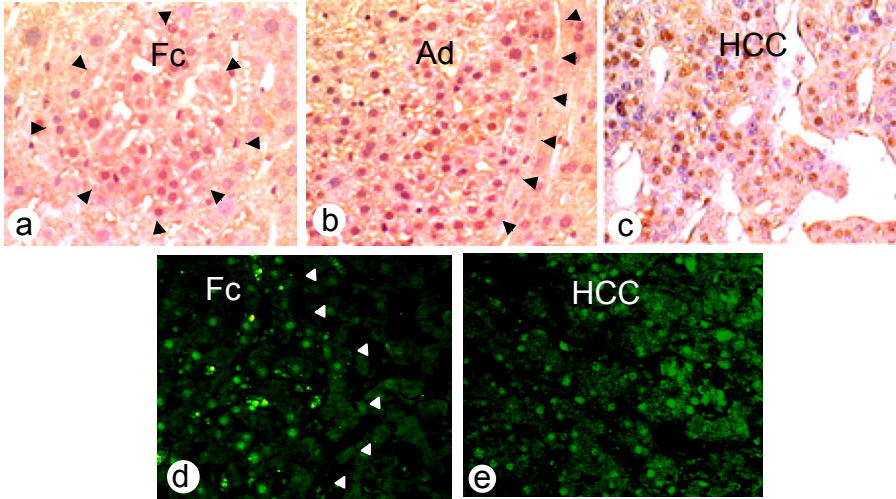


Figure 2

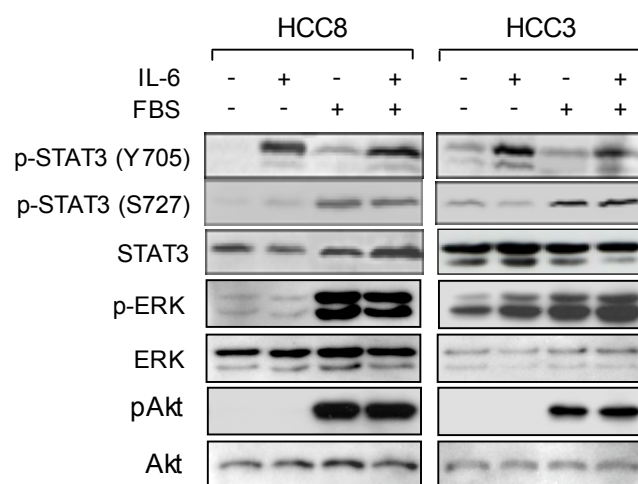


Figure 3

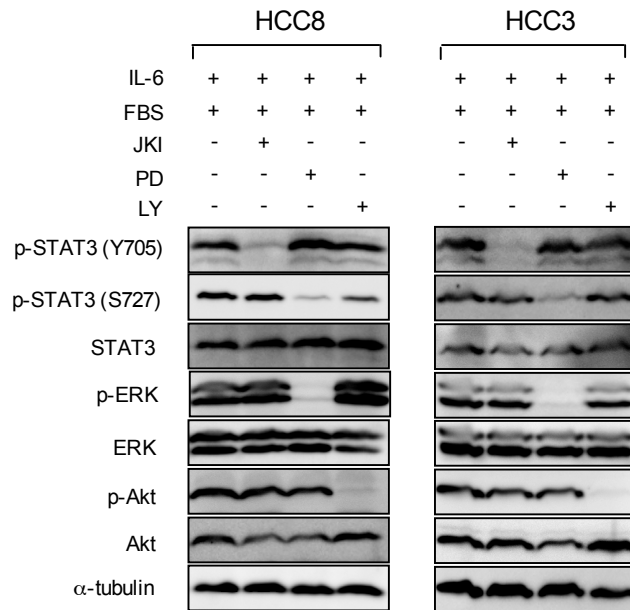
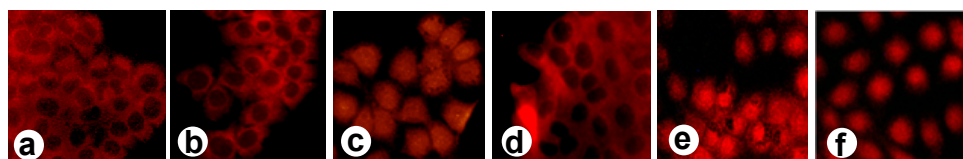


Figure 4

A



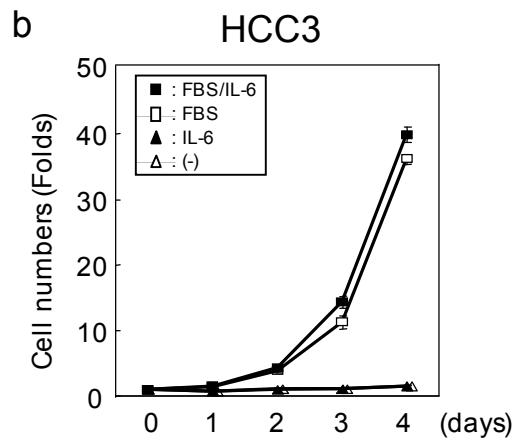
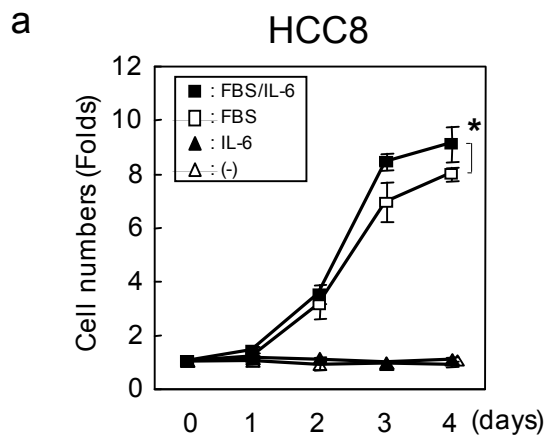
IL-6	-	+	-	-	-	-
FBS	-	-	+	+	+	+
PD	-	-	-	+	-	-
JKI	-	-	-	-	+	-
LY	-	-	-	-	-	+

B

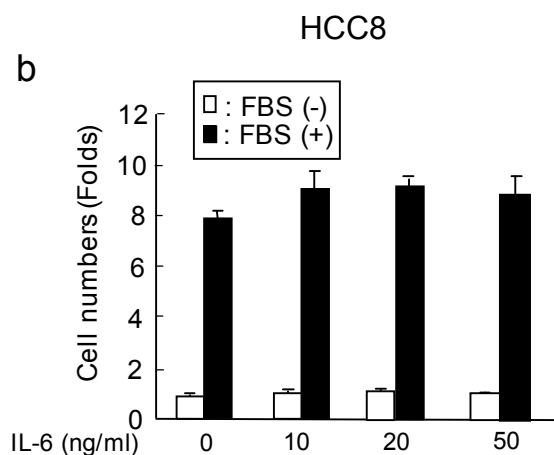
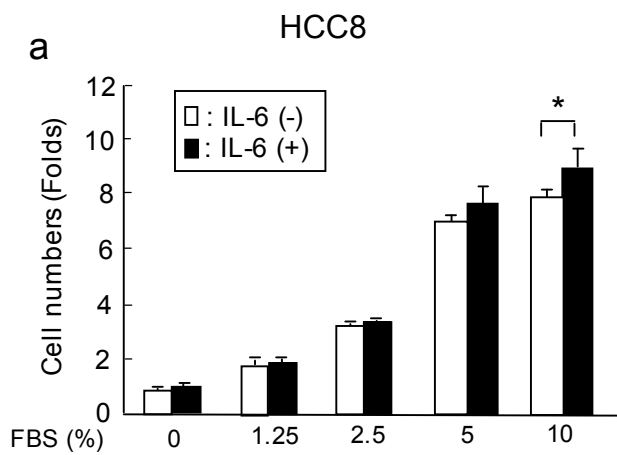
		c		n		c		n		c		n	
Total STAT3	Lamin A	[band]		[band]		[band]		[band]		[band]		[band]	
		[band]		[band]		[band]		[band]		[band]		[band]	
pY705 STAT3		[band]		[band]		[band]		[band]		[band]		[band]	
pS727 STAT3		[band]		[band]		[band]		[band]		[band]		[band]	
Lamin A		[band]		[band]		[band]		[band]		[band]		[band]	
IL-6		-	+	-	-	-	-	-	-	-	-	-	-
FBS		-	-	+	+	+	+	+	+	+	+	+	+
PD		-	-	-	-	+	-	-	-	-	-	-	-
JKI		-	-	-	-	-	-	+	-	-	-	-	-
LY		-	-	-	-	-	-	-	-	-	+	-	+
Nuclear STAT3/ Lamin A	Total	0.80	0.75	2.24	0.35	2.64	2.00						
	pY705	0.17	0.26	0.25	0.28	0.20	0.22						
	pS727	0.51	0.72	2.08	0.97	2.33	2.02						

Figure 5

A



B



C

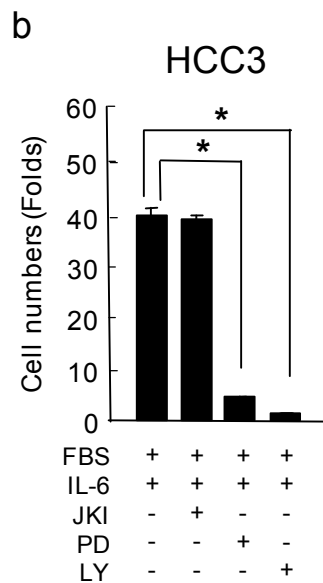
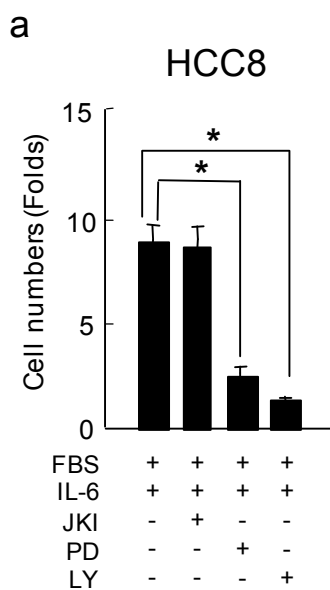
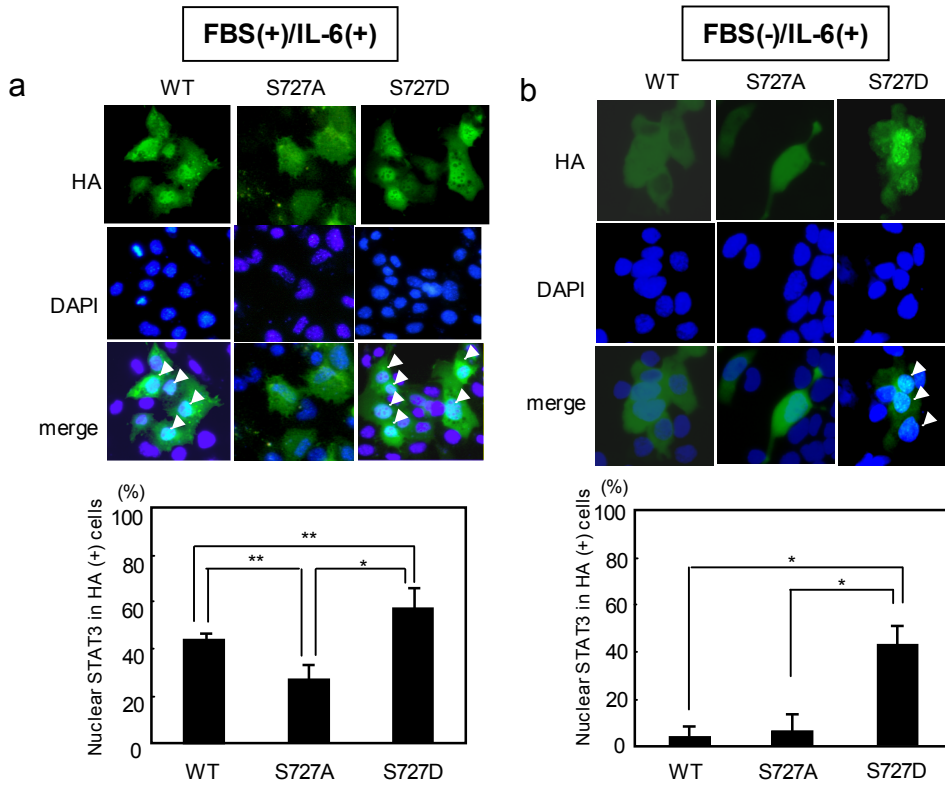


Figure 6

A



B

